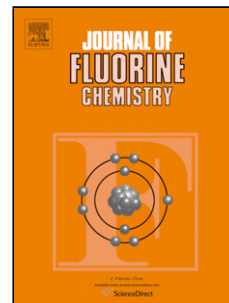


Accepted Manuscript

Title: A comparative study on the properties of aromatic polyamides with methyl- or trifluoromethyl-substituted triphenylamine groups

Author: Sheng-Huei Hsiao Kai-Han Lin



PII: S0022-1139(16)30145-2
DOI: <http://dx.doi.org/doi:10.1016/j.jfluchem.2016.06.001>
Reference: FLUOR 8786

To appear in: *FLUOR*

Received date: 28-4-2016
Revised date: 2-6-2016
Accepted date: 6-6-2016

Please cite this article as: Sheng-Huei Hsiao, Kai-Han Lin, A comparative study on the properties of aromatic polyamides with methyl- or trifluoromethyl-substituted triphenylamine groups, Journal of Fluorine Chemistry <http://dx.doi.org/10.1016/j.jfluchem.2016.06.001>

This is a PDF file of an unedited manuscript that has been accepted for publication. As a service to our customers we are providing this early version of the manuscript. The manuscript will undergo copyediting, typesetting, and review of the resulting proof before it is published in its final form. Please note that during the production process errors may be discovered which could affect the content, and all legal disclaimers that apply to the journal pertain.

**A comparative study on the properties of aromatic
polyamides with methyl- or
trifluoromethyl-substituted triphenylamine groups**

Sheng-Huei Hsiao*¹, Kai-Han Lin²

¹ *Department of Chemical Engineering and Biotechnology, National Taipei University*

of Technology, Taipei, Taiwan

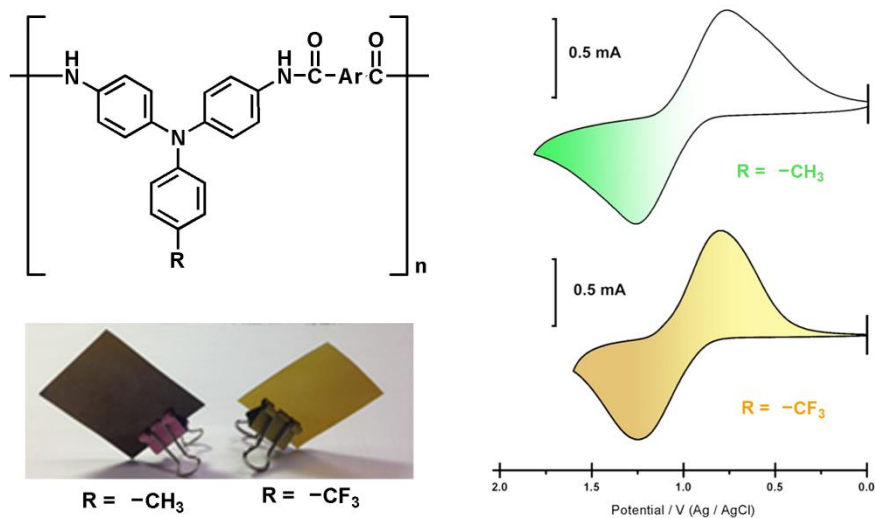
² *Department of Chemical Engineering, Tatung University, Taipei, Taiwan*

*Corresponding author.

E-mail: shhsiao@ntut.edu.tw (S.-H. Hsiao)

Graphical Abstract-Pictogram

Redox-Active and Electrochromic Aramids



A new fluorine-containing, triphenylamine-based diamine monomer, 4,4'-diamino-4''-(trifluoromethyl)triphenylamine, was synthesized and led to a series of electroactive aromatic polyamides. The electrochemical and electrochromic properties of the polyamides were investigated and compared with the those of analogous polyamides based on 4,4'-diamino-4''-methyltriphenylamine.

Highlights

- Two triphenylamine-based diamine monomers with methyl or trifluoromethyl substituent have been synthesized.
- New redox-active and electrochromic polyamides with either 4-methyltriphenylamine or 4-(trifluoromethyl)triphenylamine units were prepared.
- The polyamides showed green or dark golden coloring upon oxidation.
- Effects of the $-CF_3$ substituent on the properties of the polyamides have been investigated.

ABSTRACT

Two triphenylamine-based diamine monomers, 4,4'-diamino-4''-methyltriphenylamine and 4,4'-diamino-4''-(trifluoromethyl)triphenylamine, were synthesized via the cesium fluoride-mediated double *N*-arylation reactions of *p*-toluidine and *p*-(trifluoromethyl)aniline, respectively, with *p*-fluoronitrobenzene, followed by palladium-catalyzed hydrazine reduction of the dinitro intermediates. New redox-active aromatic polyamides containing main-chain triphenylamine unit with methyl or trifluoromethyl ($-CF_3$) group on the pendent phenyl ring were prepared by the phosphorylation polycondensation reactions of the synthesized diamine monomers with commercially available aromatic dicarboxylic acids. The polyamides were readily soluble in polar organic solvents and could afford flexible and strong films via solution casting. Cyclic voltammograms of the polyamide films cast onto the indium-tin oxide (ITO)-coated glass substrate revealed reversible electrochemical oxidation processes accompanied with color change from pale yellow to dark golden or green. Comparative studies of the methyl and $-CF_3$

substituents on the properties of the polyamides, such as solubility, thermal, electrochemical and electrochromic properties, are investigated.

Keywords: Fluorinated polyamides, Triphenylamine, Trifluoromethyl, Electrochemistry, Electrochromism, Redox polymers

1. Introduction

Wholly aromatic polyamides (aramids) are a kind of high performance polymers owing to their high mechanical properties, good chemical resistance, and excellent thermal stability [1–3]. However, the main problem of aramids is associated with their insolubility due to their rigid backbones and strong interchain interactions, leading to processing difficulties. Therefore, many efforts have been made to increase the solubility and processability of aramids through structural modification of their monomers [4–11]. One of the common approaches to increasing solubility without much compromising their thermal and mechanical stability is the use of monomers with bulky packing-disruptive moieties [12–16]. Introduction of trifluoromethyl ($-\text{CF}_3$) groups into aramids has been one of the most widely used strategies for structural modification leading to substantial solubility enhancement [17–21]. Moreover, the incorporation of bulky groups increases the interchain spacing and reduces the packing efficiency thereby increasing the intrinsic microporosity. This ultimate behavior finds application in gas separation membrane technology, where much effort has been focused to enhance gas permeability through an increment in intrinsic microporosity which could be achieved by chemical modification of the polymer chain [22–24].

Triphenylamine (TPA) derivatives and polymers are well-known for their

electroactive and photoactive properties that may find optoelectronic applications in electrophotography, electroluminescent diodes, field-effect transistors, solar cells, memory devices, and electrochromic or electrofluorochromic devices [25–33]. TPAs can be easily oxidized to form stable radical cations as long as the *para*-position of the phenyl rings is protected, and the oxidation process is always associated with a strong change of coloration. During the past decade, a huge number of high-performance polymers (typically, aromatic polyamides and polyimides) carrying the redox-active TPA unit have been prepared and evaluated for electrochromic applications [34–44]. It has been demonstrated that aromatic polyamides bearing the propeller-shaped TPA unit in the backbone were amorphous and easily soluble in polar organic solvents and could be solution-cast into flexible and strong films with high thermal stability. Thus, incorporation of three-dimensional, packing-disruptive TPA units into the aramid backbone not only resulted in enhanced solubility but also led to new electronic functions of aramids such as electrochromic characteristics.

As reported in the pioneering works by Nelson and Adams et al. [45,46], unsubstituted TPA undergoes dimerization to tetraphenylbenzidine (TPB) after the formation of an unstable monocation radical. This is accompanied by the loss of two protons per dimer and the dimer is more easily oxidized than TPA and also can undergo further oxidations in two discrete one-electron steps to give $TPB^{+\bullet}$ and finally the quinoidal TPB^{+2} . Quantitative data have been obtained for several 4-substituted TPAs in the form of second-order coupling rate constants, and it was generally found that electron-donating substituents such as methoxy group tended to stabilize the cation radicals while electron-withdrawing groups such as nitro group had the opposite effect [47]. As a continuation of our efforts in developing TPA-functionalized high performance polymers, herein we synthesize two

TPA-based diamine monomers, 4,4'-diamino-4''-methyltriphenylamine and 4,4'-diamino-4''-(trifluoromethyl)triphenylamine, and their derived aromatic polyamides containing the electroactive TPA unit with electron-donating $-\text{CH}_3$ group or electron-withdrawing $-\text{CF}_3$ group *para* substituted on the pendent phenyl ring. The effect of incorporating the $-\text{CH}_3$ and $-\text{CF}_3$ substituents on the thermal, electrochemical and electrochromic properties of the polyamides will be investigated.

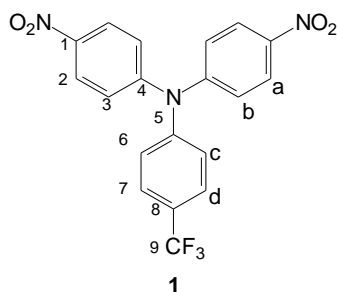
2. Experimental section

2.1 Materials

p-Toluidine (TCI), *p*-(trifluoromethyl)aniline (TCI), *p*-fluoronitrobenzene (Acros), 10 % palladium on charcoal (Pd/C, Fluka), cesium fluoride (CsF, Acros), triphenyl phosphite (TPP, TCI), and hydrazine monohydrate (Acros) were used without further purification. Pyridine (Py; Wako) and *N*-methyl-2-pyrrolidone (NMP; Fluka) were dried over calcium hydride for 24 h, distilled under reduced pressure, and stored over 4 Å molecular sieves in sealed bottles. The commercially available aromatic dicarboxylic acids including terephthalic acid (**5a**, Wako), isophthalic acid (**5b**, Wako), 4,4'-biphenydicarboxylic acid (**5c**, TCI), 4,4'-dicarboxydiphenyl ether (**5d**, TCI), bis(4-carboxyphenyl) sulfone (**5e**, New Japan Chemicals Co.), 2,2-bis(4-carboxyphenyl)hexafluoropropane (**5f**, TCI), 1,4-naphthalenedicarboxylic acid (**5g**, Wako), and 2,6-naphthalenedicarboxylic acid (**5h**, TCI) were used as received.

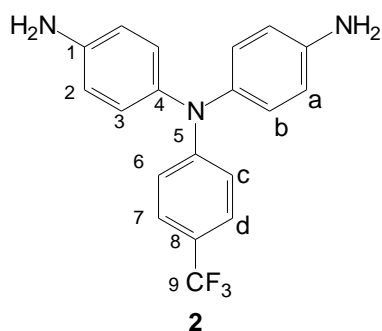
2.2 Synthesis of TPA-diamine monomers

4,4'-Dinitro-4''-(trifluoromethyl)triphenylamine (1). In a 250 mL round-bottom flask equipped with a stirring bar, a mixture of 11.3 g (0.07 mol) of *p*-(trifluoromethyl)aniline, 19.8 g (0.14 mol) of *p*-fluoronitrobenzene, and 24.3 g of CsF in 120 mL of dimethyl sulfoxide (DMSO) was heated at 120 °C for about 48 h. After cooling, the mixture was poured into 500 mL of water, and the precipitate was collected by filtration and washed thoroughly with methanol and water. The crude product was washed several times with methanol and water to afford 25.0 g (yield 88 %) of dinitro compound **1** as yellow solid, which could be further recrystallized from *N,N*-dimethylformamide (DMF)/methanol to afford yellow crystals with a melting point of 294 °C (by DSC, 2 °C/min). ANAL. Calcd for C₁₉H₁₂F₃N₃O₄ (403.31): C, 56.58%; H, 3.00%; N, 10.42%. Found: C, 56.42%; H, 2.81%; N, 10.46%. IR (KBr): 1586, 1323 (–NO₂), 1117 cm^{–1} (C–F stretch). ¹H NMR (500 MHz, DMSO-*d*₆, δ, ppm): 8.34 (d, *J* = 9.1 Hz, 4H, H_a), 7.37 (d, *J* = 9.1 Hz, 4H, H_b), 7.29 (d, *J* = 9.1 Hz, 2H, H_c), 8.23 (d, *J* = 9.1 Hz, 2H, H_d). ¹³C NMR (125 MHz, DMSO-*d*₆, δ, ppm): 160.75 (C⁵), 151.50 (C¹), 144.02 (C⁴), 143.13 (C⁷), 126.85 (C⁸, quartet, ²*J*_{C–F} = 30 Hz), 126.76 (C²), 124.68 (C⁹, quartet, ¹*J*_{C–F} = 254 Hz), 120.03 (C³).

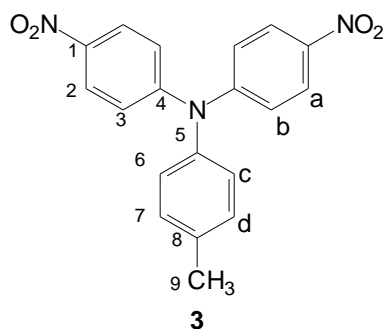


4,4'-Diamino-4''-(trifluoromethyl)triphenylamine (2). In a 500-mL round-bottom flask equipped with a stirring bar, a mixture of 10.0 g (0.025 mol) of dinitro

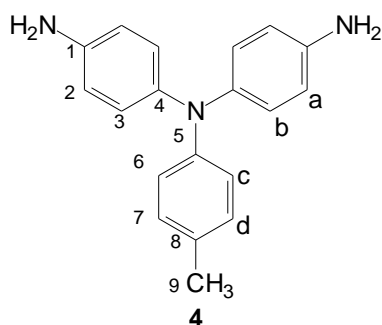
compound **1**, 0.2 g of 10% Pd/C, 7.5 mL of hydrazine monohydrate, and 150 mL of ethanol was heated at reflux for 10 h. The solution was filtered to remove Pd/C catalyst, and the filtrate was distilled to remove the solvent. The residue was washed with water and dried in vacuo at 100 °C to give 8.6 g (yield: 95%) of grey product; the crude product was further recrystallized from ethanol to afford grey crystals with a melting point of 114 °C (by DSC, 2 °C/min). ANAL. Calcd for C₁₉H₁₆F₃N₃ (343.35): C, 66.47%; H, 4.70%; N, 12.24%. Found: C, 66.35%; H, 4.78%; N, 12.35%. IR (KBr): 3474, 3379 cm⁻¹ (-NH₂ stretch), 1114 cm⁻¹ (C-F stretch). ¹H NMR (500 MHz, DMSO-*d*₆, δ, ppm): 7.35 (d, *J* = 8.9 Hz, 2H, H_d), 6.93 (d, *J* = 8.6 Hz, 4H, H_b), 6.67 (d, *J* = 8.9 Hz, 2H, H_c), 6.65 (d, *J* = 8.6 Hz, 2H, H_a), 5.11 (s, 4H, -NH₂) . ¹³C NMR (125 MHz, DMSO-*d*₆, δ, ppm) : 152.88 (C⁵), 146.77 (C¹), 134.81 (C⁴), 128.28 (C³), 126.15 (C⁷), 125.34 (C⁹, quartet, ¹*J*_{C-F} = 270 Hz), 116.93 (C⁸, quartet, ²*J*_{C-F} = 31 Hz), 115.32 (C²), 114.59 (C⁶).



4,4'-Dinitro-*4''*-methyltriphenylamine (**3**). The compound **3** was prepared by a similar procedure described for the synthesis of compound **1**, except that *p*-toluidine was used instead of *p*-(trifluoromethyl)aniline; mp = 249 °C (by DSC, 2 °C/min). IR (KBr): 1579, 1339 cm⁻¹ (-NO₂). ¹H NMR (500 MHz, DMSO-*d*₆, δ, ppm): 8.18 (d, *J* = 9 Hz, 4H, H_a), 7.22 (d, *J* = 9 Hz, 2H, H_d), 7.18 (d, *J* = 9 Hz, 4H, H_b), 7.08 (d, *J* = 9 Hz, 4H, H_c). ¹³C NMR (125 MHz, DMSO-*d*₆, δ, ppm): 158.51 (C⁵), 152.03 (C¹), 141.98 (C⁴), 137.13 (C⁷), 129.53 (C⁸), 125.82 (C²), 122.04 (C³), 116.16 (C⁶), 51.71 (C⁹).



4,4'-Diamino-4''-methyltriphenylamine (4). The diamine monomer **4** was prepared by the Pd/C-catalyzed reduction of dinitro compound **3** using the similar procedure described for the synthesis of **2**; mp = 146 °C (by DSC, 2 °C/min). IR (KBr): 3454, 3338 cm⁻¹ (-NH₂ stretch). ¹H NMR (500 MHz, DMSO-*d*₆, δ, ppm): 6.90 (d, *J* = 8.5 Hz, 2H, H_d), 6.76 (d, *J* = 8.5 Hz, 4H, H_b), 6.59 (d, *J* = 8.5 Hz, 2H, H_c), 6.55 (d, *J* = 8.5 Hz, 4H, H_a) 4.88 (s, 4H, -NH₂). ¹³C NMR (125 MHz, DMSO-*d*₆, δ, ppm): 147.00 (C⁵), 145.02 (C¹), 137.21 (C⁴), 129.49 (C⁷), 127.48 (C⁸), 127.48 (C³), 118.44 (C⁶), 115.28 (C²), 20.34 (C⁹).



2.3 Polymer synthesis

The Yamazaki-Higashi phosphorylation polycondensation technique [48] was used to prepare the polyamides. A typical example for the preparation of polyamide **6a** is given. A flask was charged with 0.5150 g (1.5 mmol) of diamine monomer **2**,

0.2492 g (1.5 mmol) of terephthalic acid (**5a**), 0.2 g of CaCl₂, 1.5 mL of TPP, 0.5 mL pyridine, and 3 mL of NMP. This mixture was heated with stirring at 120 °C for 3 h. The resulting viscous polymer solution was poured slowly into 300 mL of methanol with stirring. The fiber-like precipitate was filtered off, washed thoroughly with methanol and hot water, and dried. The inherent viscosity of polyamide **6a** was 0.98 dL/g, as measured at a concentration of 0.5 dL/g in *N,N*-dimethylacetamide (DMAc) at 30 °C.

2.4 Instrumentation and measurements

Infrared spectra were recorded on a PerkinElmer FT-IR System spectrum GX. ¹H and ¹³C NMR spectra were obtained on a Bruker AV-500 FT NMR spectrometer. The inherent viscosities of the polyamides were determined with a Cannon-Fenske viscometer at 30 °C. Weight-average molecular weights and number-average molecular weights were obtained via size exclusion chromatography (SEC) on the basis of polystyrene calibration using Water 2410 apparatus and tetrahydrofuran (THF) as the eluent. A universal tester LLOYD LRX with a load cell of 5 kg was used to study the stress-strain behavior of the samples. A gauge length of 2 cm and a crosshead speed of 5 mm/min were used for this study. Measurements were performed at room temperature with film specimens (0.5 cm wide, 6 cm long, and about 0.09 mm thick), and an average of at least three replicates was used. Wide-angle X-ray diffraction (WAXD) measurements were performed at room temperature (ca. 25 °C) on a Shimadzu XRD-6000 X-ray diffractometer (operating at 40 kV and 30 mA) with graphite-monochromatized Cu K α radiation ($\lambda = 1.5418 \text{ \AA}$). The scanning rate was 2 °/min over a range of $2\theta = 10\text{--}40^\circ$. Thermogravimetric analysis (TGA) was conducted with a PerkinElmer Pyris 1 TGA. Experiments were

carried out on approximately 4–8 mg of samples in flowing nitrogen (flow rate 30 cm³/min) at a heating rate of 20 °C/min. Thermomechanical analysis (TMA) was conducted with a PerkinElmer TMA 7 instrument. The TMA experiments were conducted from 50 °C to 350 °C at a scanning rate of 10 °C/min by using a penetration probe 1.0 mm in diameter under an applied constant load of 10 mN. Softening temperatures (T_s) were taken as the onset temperature of probe displacement on the TMA traces. Electrochemistry was performed with a Bioanalytical System model CV-27 potentiostat and a BAS X-Y recorder. Voltammograms are presented with the positive potential pointing to the left and with increasing anodic currents pointing downward. Cyclic voltammetry was conducted with the use of a three-electrode cell in which ITO (the polymer film area was ca. 0.7 cm x 0.5 cm) was used as a working electrode. A platinum wire was used as an auxiliary electrode. All cell potentials were taken with the use of a homemade Ag/AgCl, KCl (saturated) reference electrode. The spectroelectrochemical cell was composed of a 1-cm cuvette, ITO as a working electrode, a platinum wire as an auxiliary electrode, and an Ag/AgCl reference electrode. Absorption spectra were measured with an Agilent 8453 UV-vis spectrophotometer.

3. Results and discussion

3.1. Monomer synthesis

The TPA-based diamine monomers **2** and **4** were prepared by the synthetic routes outlined in Scheme 1. The first step involved a nucleophilic aromatic

fluoro-displacement of *p*-fluoronitrobenzene with *p*-(trifluoromethyl)aniline and *p*-toluidine, respectively, in the presence of CsF in DMSO. Diamines **2** and **4** were readily obtained in high yields by the Pd/C-catalyzed reduction of the intermediate dinitro compounds **1** and **3** with hydrazine monohydrate in refluxing ethanol. The structures of dinitro precursors and the target diamine monomers were confirmed by elemental analyses as well as FTIR and NMR spectroscopy.

FTIR spectra of all the synthesized compounds are included in the supplementary data (Fig. S1). The nitro group of **1** and **3** gave two characteristic bands around 1585 and 1325 cm^{-1} , which disappeared after reduction. The diamine monomers **2** and **4** showed a typical $-\text{NH}_2$ stretching absorption pair in the region of 3300-3500 cm^{-1} . The ^1H NMR and ^{13}C NMR spectra of diamines **2** and **4** are illustrated in Fig. 1 and Fig. 2, respectively. The ^1H NMR spectra of diamines **2** and **4** confirmed that the signals at 5.11 and 4.88 ppm corresponding to the primary aromatic amine protons. All the ^{13}C atoms in diamine **2** resonated in the region 100–150 ppm, and the quartets centered at about 125.34 ppm due to the $-\text{CF}_3$ carbons. The one-bond C–F coupling constant was about 270 Hz. The methyl carbons in diamine **4** showed a singlet at 20.34 ppm in its ^{13}C NMR spectrum. The assignments of each carbon and proton are also given in the figures, which agree well with the expected structures of diamine monomers **2** and **4**.

3.2. Polymer synthesis

According to the phosphorylation polyamidation technique developed by Yamazaki and his co-workers [48], two series of aromatic polyamides **6a–h** and **7a–h** were synthesized from the diamine monomers **2** and **4** with various aromatic dicarboxylic acids **5a–h** via solution polycondensation using TPP and pyridine as condensing agents in the NMP solution containing dissolved CaCl_2 (Scheme 2). All the polymerization reactions proceeded homogeneously throughout the reaction and afforded clear and highly viscous polymer solutions. The polymer products precipitated in a tough, fiber-like form when the resulting polymer solutions were slowly pouring into stirring methanol. As shown in Table 1, the obtained polyamides exhibited inherent viscosities in the range of 0.42–1.31 dL/g and could be solution-cast into creasable, strong films from DMAc solutions, indicating high-molecular-weight polymers. The THF-soluble polyamide **6f** showed a weight-average molecular weight (Mw) and number-average molecular weight (Mn) of 41000 and 31000, respectively, on the basis of SEC. Fig. S2 (Supplementary data) shows a typical IR spectrum for polyamide **6a**. The characteristic IR absorption bands of amide group can be found at around 3288 cm^{-1} (N-H stretching) and 1654 cm^{-1} (amide carbonyl).

3.3. Solubility and film properties

The solubility behaviors of all polyamides are reported in Table 1. All the polyamides **6a–h** and **7a–h** were highly soluble in the polar organic solvents such as NMP, DMAc, DMF, and DMSO. The high solubility of these polyamides is apparently due to the presence of TPA unit. The substituents on the TPA unit seem does not play a dominant role since these two series polyamides display a similar solubility behavior. Among these polyamides, polymer **6f** was soluble in all the test solvents including less polar *m*-cresol and THF. This can be attributable to the additional contribution of the hexafluoroisopropylidene [$-\text{C}(\text{CF}_3)_2-$] fragment in the polymer backbone together with the bulky $-\text{CF}_3$ substituent which interfere the interchain interactions and close chain packing. Therefore, the good solubility makes

these polyamides candidates for practical applications via solution processing techniques to afford high performance thin films for optoelectronic devices.

The WAXD patterns of polyamides **6a-h** and **7a-h** are illustrated in Fig. S3. The results indicate that all the **6** and **7** series polyamides are amorphous in nature. Thus, the amorphous nature of most **6** and **7** series polyamides also reflected in their excellent solubility and good film-forming ability. Fig. 3 shows the appearance of the DMAc-cast films of typical polyamides **6h** and **7h**. The **6** series polymers exhibited lighter color than the corresponding **7** series ones due to the bulky $-\text{CF}_3$ substituent. The mechanical properties of the polyamide films are summarized in Table 2. The polymer films had a tensile strength of 76-117 MPa, an elongation at break of 7-49%, and a tensile modulus of 1.6-2.9 GPa. Most of the polymer films exhibited high tensile strengths; thus, they could be considered as strong materials.

3.4. Thermal properties

TMA and TGA were used to investigate the thermal properties of the polyamide films, and some of the thermal behavior data are reported in Table 3. To avoid the effects of the absorbed moisture and residual solvent in the film samples, we heated the samples at 300 °C for 1 h prior to all thermal analyses. The softening temperatures (T_s) of the thoroughly dried polymer films were measured with TMA by the penetration method. They were obtained from the onset temperatures of the probe displacement on the TMA traces. As a typical example, the TMA trace of polyamide **7b** is illustrated in Fig. S4. The T_s values of these polymers were observed in the range of 259–317 °C. The lowest T_s value of **6d** and **7d** in each series polyamides can be explained in terms of the flexible ether linkage in their diacid component. In most cases, the **6** series polyamides revealed slightly lower T_s when compared to their corresponding **7** series analogs. This result implies that the bulky $-\text{CF}_3$ substituent in the **6** series polymers leads to an increase in steric hindrance for close chain packing and thus an enhanced fractional free volume.

The thermal and thermo-oxidative stability of these polyamides were measured by TGA. The temperatures of 10 % weight loss in nitrogen and air atmospheres determined from the original TGA thermograms are included in Table 3. All polymers exhibited good thermal stabilities with decomposition temperature (T_d) at 10 % weight loss above 450 °C in both

nitrogen and air atmospheres. The anaerobic char yield at 800 °C for all polymers was in the range of 65–74 wt %. All the polyamides exhibited a lower T_d as compared with their corresponding counterparts without the substituted group [49], implying that the earlier weight loss is associated with the decomposition of the substituent on the TPA unit.

3.5. Optical and electrochemical properties

The optical and electrochemical properties of the polyamides were investigated with UV–Vis absorption spectroscopy and cyclic voltammetry (CV). The relevant data are summarized Table 4. These polymers exhibited strong UV–Vis absorption bands at 300–346 nm in solid films, which were assignable to the π – π^* transitions in the backbones. The cutoff wavelengths (absorption edge) read from the UV–Vis absorption spectra are also indicated in Table 4 and were recorded in the range of 397–455 nm, dependent on the diacid component and the substituent on the TPA unit. The cutoff wavelengths (λ_{onset}) of the polyamides generally increased with increasing electron affinity of the corresponding diacid residue, and the **6** series polyamides revealed a slightly lowered λ_{onset} as compared to the corresponding **7** series polymers. This result suggests that the coloration of the polymer film was caused by charge-transfer (CT) interactions.

The redox behavior of the **6** and **7** series polyamides was investigated by CV conducted for the cast films on an ITO-coated glass substrate as the working electrode in dry acetonitrile (CH_3CN) containing 0.1 M TBAP as an electrolyte under a nitrogen atmosphere. The typical CV diagrams for polyamides **6a** and **7d** are shown in Fig. 4. There is one reversible oxidation redox couple at $E_{1/2}$ value of 1.00 V for polyamide **6a** and at $E_{1/2} = 0.84$ V for polyamide **7d** in the oxidative scan. Upon oxidation, the polymer films of **6a** and **7d** changed color from original colorless or pale yellow to dark golden and pale green, respectively. As can be seen from Table 4, the **6** series polyamides displayed a higher $E_{1/2}$ value (0.97–1.03 V) in comparison with the **7** series polyamides (0.83–0.88 V), attributable to the electron-withdrawing trifluoromethyl substituent on the TPA unit. Methyl group, on the other hand, inductively donates electrons. This is the same hyperconjugative donating effect that causes alkyl substituents to stabilize alkenes and carbocations. When compared with

the structurally related polyamides (the **8** series) based on 4-fluorotriphenylamine [50], the trifluoromethyl-substituted **6** series polymers also showed a higher oxidation potential. The withdrawal or donation of electrons by a substituent group is controlled by an interplay of inductive effects and resonance effects. The trifluoromethyl groups inductively withdraw electrons through the σ bond linked to the benzene ring and are strongly deactivating. The direct fluorine substituent is weakly deactivating owing to the interplay of inductive effects and resonance effects. The energy levels of the highest occupied molecular orbital (HOMO) and the lowest unoccupied molecular orbital (LUMO) of the corresponding polyamides were estimated from the $E_{1/2}$ values. Assuming that the HOMO energy level for the ferrocene/ferrocenium (Fc/Fc⁺) standard is 4.8 eV with respect to the zero vacuum level, the HOMO levels for these polyamides were calculated to be 5.19–5.39 eV. Their LUMO energy levels deduced from the band gap calculated from the absorption edge were 2.06–2.59 eV.

3.6. Spectroelectrochemical and electrochromic properties

The electrochromism of thin films from the polyamides was examined via the casting of polymer solutions onto an ITO-coated glass substrate, and their absorption profiles were monitored with a UV–Vis spectrometer at different applied potentials. The electrode preparation and solution conditions were identical to those used in cyclic voltammetry. The typical spectral changes of polyamide **6a** and **7d** are shown in Figs. 5 and 6, respectively. When the applied potentials increased positively from 0.71 to 1.36 V, the absorption peak of polyamide **6a** at 342 nm decreased gradually, whereas three new bands grew up at 404, 540 and 855 nm because of the electron oxidation. Meanwhile, the film color changed from pale yellow to chrome yellow or dark golden at electrode potential of 1.2 V. Upon electro-oxidation, the polymer film of **7d** showed new absorption bands at 397, 641, and 809 nm, which appeared the complementary color of pale green after oxidation.

To explore the potential application of the polyamide films as electrochromic materials, a square-wave potential step method coupled with UV-Vis spectroscopy were used to evaluate their electrochromic properties. In Fig. 7 are depicted the chronoabsorptograms obtained for polyamide **6a** film in TBAP/CH₃CN for the color change pale yellow \rightleftharpoons dark golden. The switching times estimated from the absorbance-time curves and indicated in Fig.

8 were determined by considering 90% of the full optical change. Thin films from polyamide **6a** would require 5 s for coloring after applying a voltage of 1.23 V and 2 s for bleaching after switching off the potential. Because the electron-withdrawing $-\text{CF}_3$ group destabilizes the TPA radical cation formed upon oxidation, a considerable loss of optical contrast was observed after ten redox switches for polyamide **6a**. In general, the **6** series polyamides displayed an inferior electrochromic performance as compared to the **8** series based on 4-fluorotriphenylamine [50] because of less electrochemical stability of the CF_3TPA unit. Thin films from polyamide **7d** would require 5 s for coloring (at 1.26 V) and 2 s for bleaching. After ten continuous cyclic scans between 0.0 and 1.26 V, the polyamide **7d** film still did not show significant loss in optical contrast. It is reasonable that the CH_3TPA -functionalized **7** series polyamides exhibited much better electrochromic stability than the CF_3TPA -based **6** series because the former ones formed more stable TPA radical cations in the oxidative processes. Although the CF_3TPA -based **6** series polyamides showed a less electrochromic performance, the bulkiness of the $-\text{CF}_3$ group and their good film quality make them potential application as gas separation membranes. Their other optoelectronic applications such as memory devices are still deserved to be developed.

4. Conclusions

New TPA-functionalized aromatic polyamides with $-\text{CH}_3$ or $-\text{CF}_3$ substituents were synthesized from the phosphorylation polycondensation reactions of TPA-based diamines **2** and **4** with various aromatic dicarboxylic acids. Because of the presence of the bulky, packing-disruptive TPA unit, all the polymers were amorphous, had good solubility in many polar aprotic solvents, and could afford flexible and strong films with good mechanical properties. All the polyamides had softening temperatures higher than 275 °C and high thermal stability, with 10% weight loss temperature being recorded above 450 °C in both nitrogen and air atmospheres. Introduction of electron-withdrawing $-\text{CF}_3$ group increased the oxidation potential of the polyamides and decreased the electrochemical and electrochromic stability of the polyamides. The CH_3TPA -containing polyamides exhibited good redox stability and might be good candidates for electrochromic applications.

Acknowledgement

The authors thank the Ministry of Science and Technology, Taiwan for the financial support (Grant No. MOST 104-2221-E-027-106).

Appendix A. Supplementary data

Supplementary data associated with this article can be found, in the online version, at <http://dx.doi.org/10.1016/j.jfluchem.2016.xx.xxx>.

References

1. P.E. Cassidy PE, *Thermally Stable Polymers*. Marcel Dekker, New York, 1980.
2. H.H. Yang, *Aromatic High-Strength Fibers*. Wiley, New York, 1989, pp. 66-289.
3. H.H. Yang, *Kevlar Aramid Fiber*. Wiley, New York, 1993.
4. Y. Imai, *High Perform. Polym.* 7 (1995) 337–345.
5. Y. Imai, *React. Funct. Polym.* 30 (1996) 3–15.
6. S.H. Hsiao, P.C. Huang PC, *J. Polym. Sci. Part A: Polym. Chem.* 35 (1997) 2421–2429.
7. G.C. Eastmond, J. Paprotny, R.S. Irwin RS, *Polymer* 40 (1999) 469–486.
8. J.F. Espeso, E. Ferrero, J.C. de la Campa, A.E. Lozano, J. de Abajo, *J. Polym. Sci. Part A: Polym. Chem.* 39 (2001) 475–485.
9. S.-H. Hsiao, Y.-H. Chang, *Eur. Polym. J.* 40 (2004) 1749–1757.
10. M. Ghaemy, S.M. Amini Nasab, *React. Funct. Polym.* 70 (2010) 306–313.
11. J.M. Garcia, F.C. Garcia, F. Serna, J.L. de la Pena, *Prog. Polym. Sci.* 35 (2010) 623–686.
12. G.-S. Liou, S.-H. Hsiao, *J. Polym. Sci. Part A: Polym. Chem.* 40 (2002) 1781–1789.
13. G.-S. Liou GS, S.-H. Hsiao, M. Ishida, M. Kakimoto, Y. Imai, *J. Polym. Sci. Part A: Polym. Chem.* 40 (2002) 2810–2818.
14. S.-H. Hsiao, W.-T. Chen, *J. Polym. Sci. Part A: Polym. Chem.* 41 (2003) 420–431.
15. S.-H. Hsiao, Y.-M. Chang, *J. Polym. Sci. Part A: Polym. Chem.* 42 (2004) 4056–4062.
16. H. Behniafar, S. Khosravi-born, *Polym. Int.* 58 (2009) 1299–1307.
17. S.-R. Sheng, X.-L. Pei, Z.-Z. Huang, X.-L. Liu, C.-S. Song, *Eur. Polym. J.* 45 (2009) 230–236.
18. S.-H. Hsiao, W.-J. Guo, C.-L. Chung, W.-T. Chen, *Eur. Polym. J.* 46 (2010) 1878–1890.
19. H. Behniafar, M. Sedaghatdoost, *J. Fluorine Chem.* 132 (2011) 276–284.

20. M. Ghaemy, F.R. Berenjestanaki, *J. Fluorine Chem.* 144 (2014) 86–93.
21. X.-L. Liu, D. Wu, R. Sun, L.-M. Yu, J.-W. Jiang, S.-R. Sheng, *J. Fluorine Chem.* 154 (2013) 16–22.
22. P. Bandyopadhyay, D. Bera, S. Ghosh, S. Banerjee, *RSC Adv.* 4 (2014) 28078–28092.
23. D. Bera, V. Padmanabhan, S. Banerjee, *Macromolecules* 48 (2015) 4541–4554.
24. D. Bera, P. Bandyopadhyay, S. Ghosh, S. Banerjee, V. Padmanabhan, *J. Membr. Sci.* 474 (2015) 20–31.
25. M. Thelakkat, *Macromol. Mater. Eng.* 287 (2002) 442–461.
26. Y. Shirota, H. Kageyama, *Chem. Rev.* 107 (2007) 953–1010.
27. Z. Ning, H. Tian, *Chem. Commun.* (2009) 5483–5495.
28. A. Iwan, D. Sek, *Prog. Polym. Sci.* 36 (2011) 1277–1325.
29. H.-J. Yen, G.-S. Liou, *Polym. Chem.* 3 (2012) 255–264.
30. M. Liang, J. Chen, *Chem. Soc. Rev.* 42 (2013) 3453–3488.
31. W.-P. Lin, S.-J. Liu, T. Gong, Q. Zhao, W. Huang, *Adv. Mater.* 26 (2014) 570–606.
32. J.-H. Wu, G.-S. Liou, *Adv. Funct. Mater.* 24 (2014) 6422–6429.
33. H.-J. Yen, G.-S. Liou, *Polym. J.* 48 (2016) 117–138.
34. S.-H. Cheng, S.-H. Hsiao, T.-H. Su, G.-S. Liou, *Macromolecules* 38 (2005) 307–316.
35. S.-H. Hsiao, Y.-M. Chang, H.-W. Chen, G.-S. Liou, *J. Polym. Sci. Part A: Polym. Chem.* 44 (2016) 4579–4592.
36. C.-W. Chang, G.-S. Liou, S.-H. Hsiao, *J. Mater. Chem.* 17 (2007) 1007–1015.
37. S.-H. Hsiao, G.-S. Liou, Y.-C. Kung, H.-J. Yen, *Macromolecules* 41 (2008) 2800–2808.
38. H.-J. Yen, G.-S. Liou, *Chem. Mater.* 21 (2009) 4062–4070.
39. Y.-C. Kung, S.-H. Hsiao, *J. Mater. Chem.* 20 (2010) 5841–5849.
40. L.-T. Huang, H.-J. Yen, G.-S. Liou, *Macromolecules* 44 (2011) 9595–9610.
41. H.-J. Yen, K.-Y. Lin, G.-S. Liou, *J Polym Sci Part A: Polym Chem* 50 (2012) 61–69.
42. S.-H. Hsiao, H.-M. Wang, P.-C. Chang, Y.-R. Kung, T.-M. Lee, *J. Polym. Res.* 20 (2013) 154.
43. H.-M. Wang, S.-H. Hsiao, *J. Polym. Sci. Part A: Polym. Chem.* 52 (2014) 272–286.
44. S.-H. Hsiao, S.-L. Cheng, *J. Polym. Sci. Part A: Polym. Chem.* 53 (2015) 496–510.
45. E.T. Seo, R.F. Nelson, J.M. Fritsch, L.S. Marcoux, D.W. Leedy, R.N. Adams, *J. Am. Chem. Soc.* 88 (1966) 3498–3503.
46. R.F. Nelson, R.N. Adams, *J. Am. Chem. Soc.* 90 (1968) 3925–3930.
47. S.C. Creason, J. Wheeler, R.F. Nelson, *J. Org. Chem.* 37 (1972) 4440–4446.

48. N. Yamazaki, M. Matsumoto, F. Higashi, *J. Polym. Sci. Polym. Chem. Ed.* 13 (1975) 1373–1380.
49. Y.-C. Kung, G.-S. Liou, S.-H. Hsiao, *J. Polym. Sci. Part A: Polym. Chem.* 47 (2009) 1740–1755.
50. S.-H. Hsiao, Y.-R. Kung, *J. Fluorine Chem.* 186 (2016) 79–90.

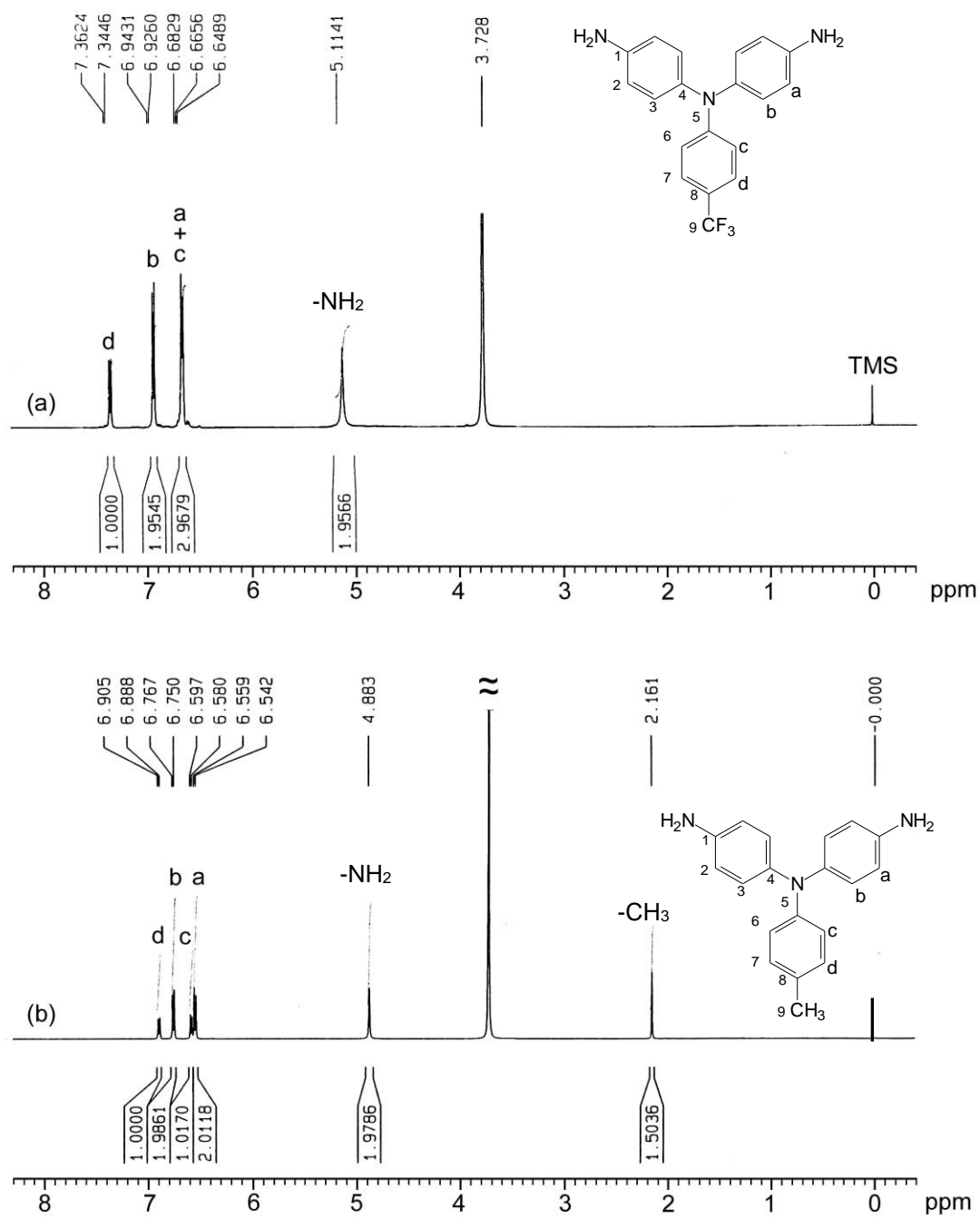


Fig. 1. ¹H NMR spectra of (a) diamine **2** and (b) diamine **4** in DMSO-*d*₆.

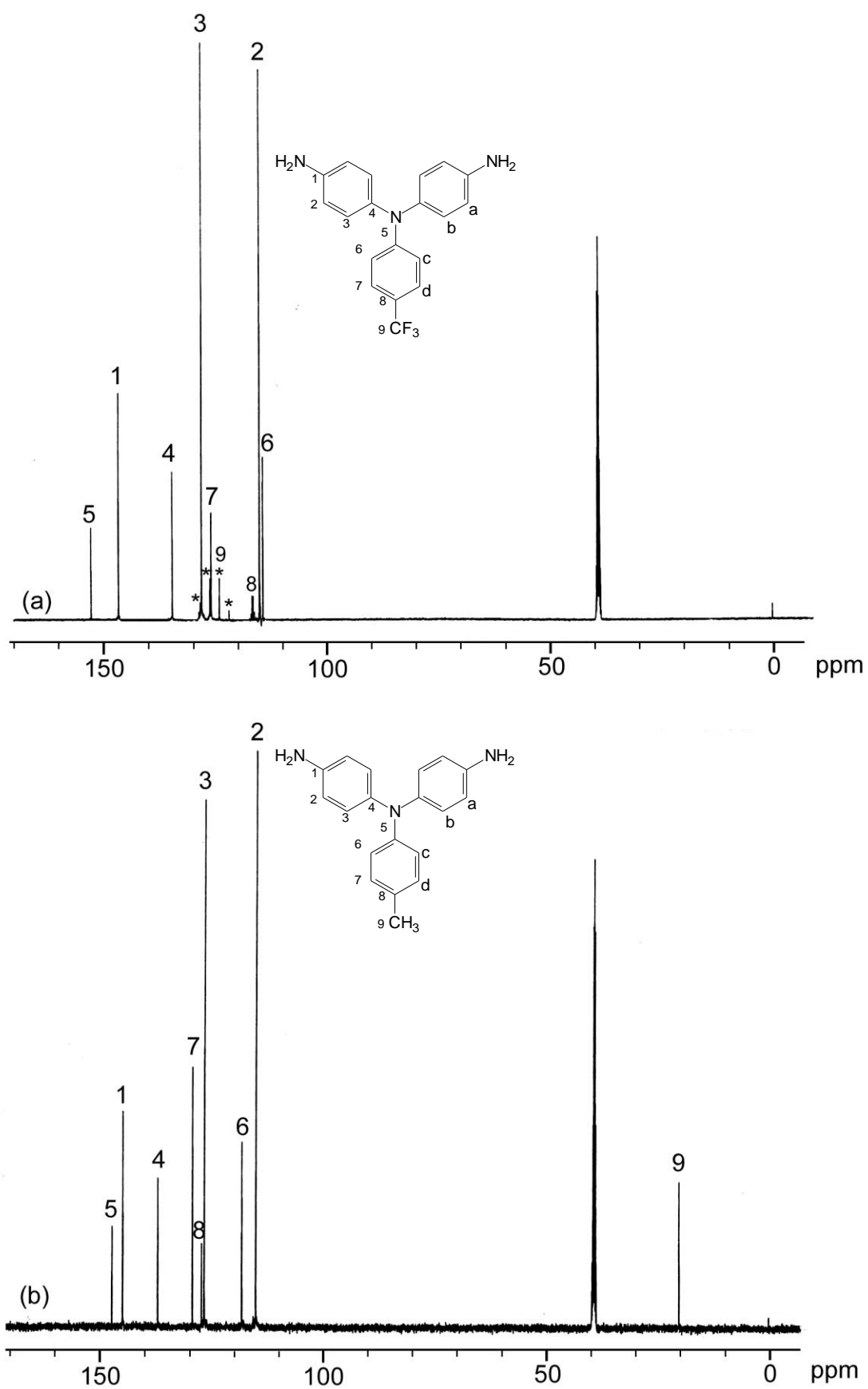


Fig. 2. ^{13}C NMR spectra of (a) diamine 2 and (b) diamine 4 in $\text{DMSO-}d_6$.

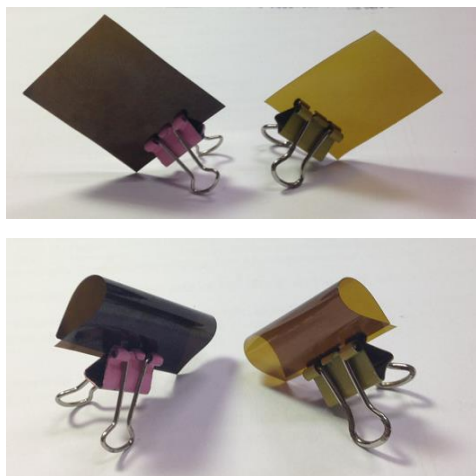


Fig. 3. Typical DMAC-cast films of polyamides **6h** (right) and **7h** (left).

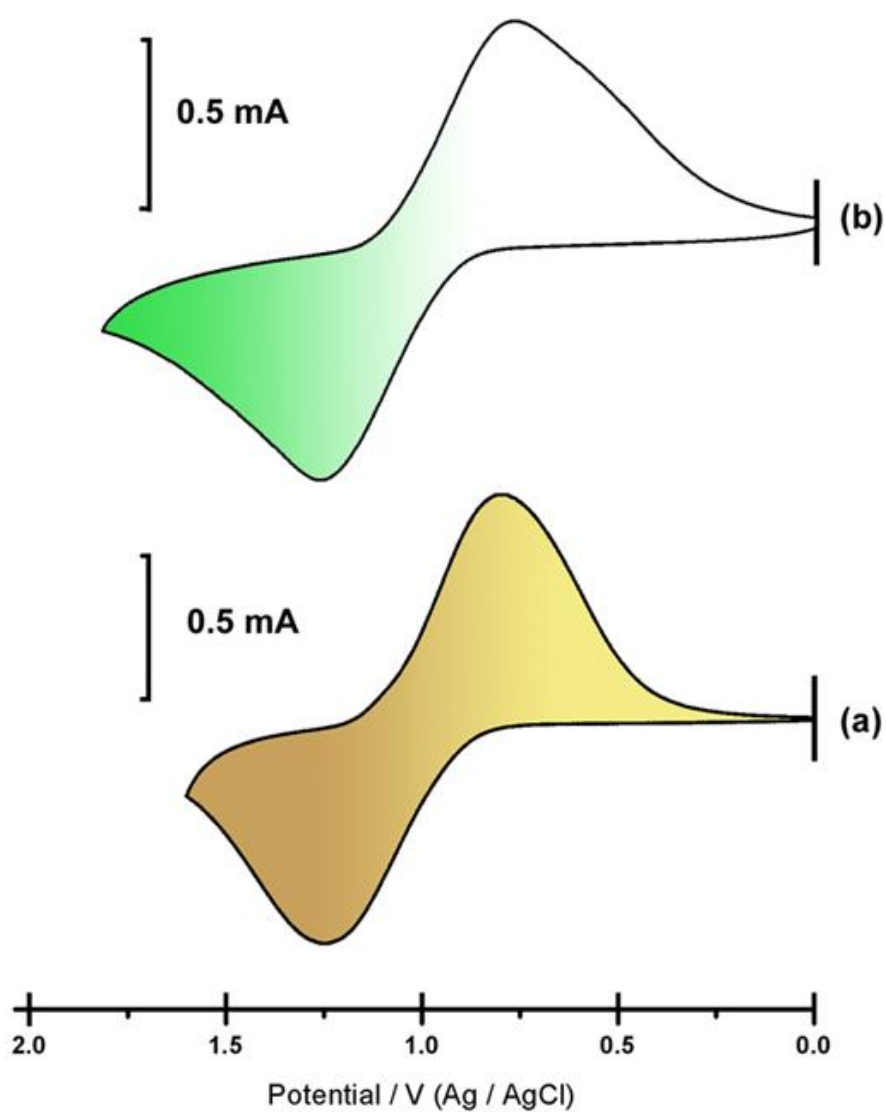


Fig. 4. Cyclic voltammograms of the cast films of polyamides (a) **6a** and (b) **7d** on an indium-tin oxide (ITO)-coated glass substrate in 0.1 M TBAP/CH₃CN at a scan rate of 100 mV/s.

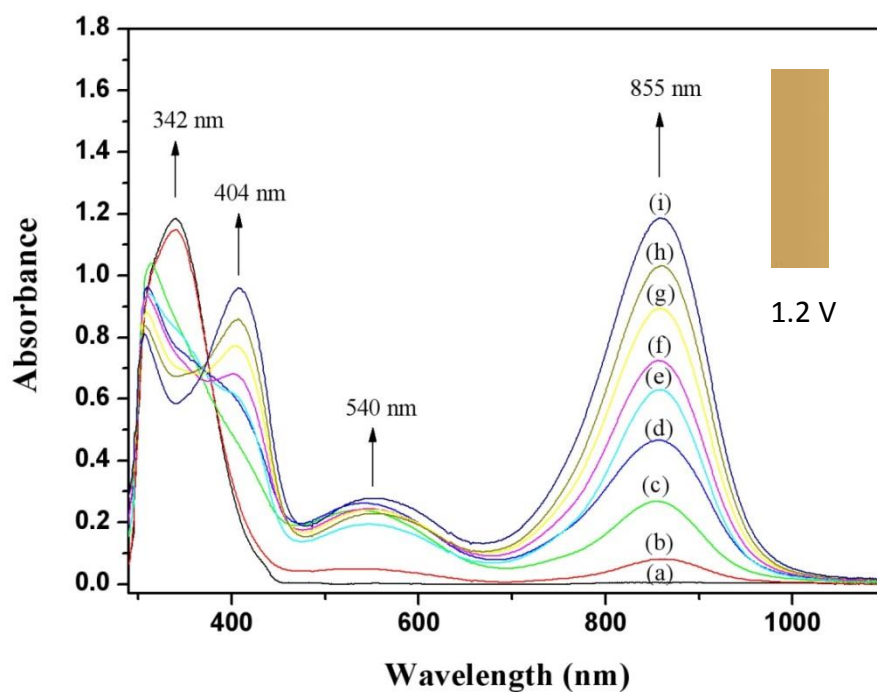


Fig. 5. Spectral changes of polyamide **6a** film on the ITO-glass substrate in 0.1 M TBAP/CH₃CN at different electrode potentials: (a) 0.0, (b) 0.71, (c) 0.78, (d) 0.85, (e) 0.92, (f) 1.00, (g) 1.08, (h) 1.15, and (i) 1.23 V.

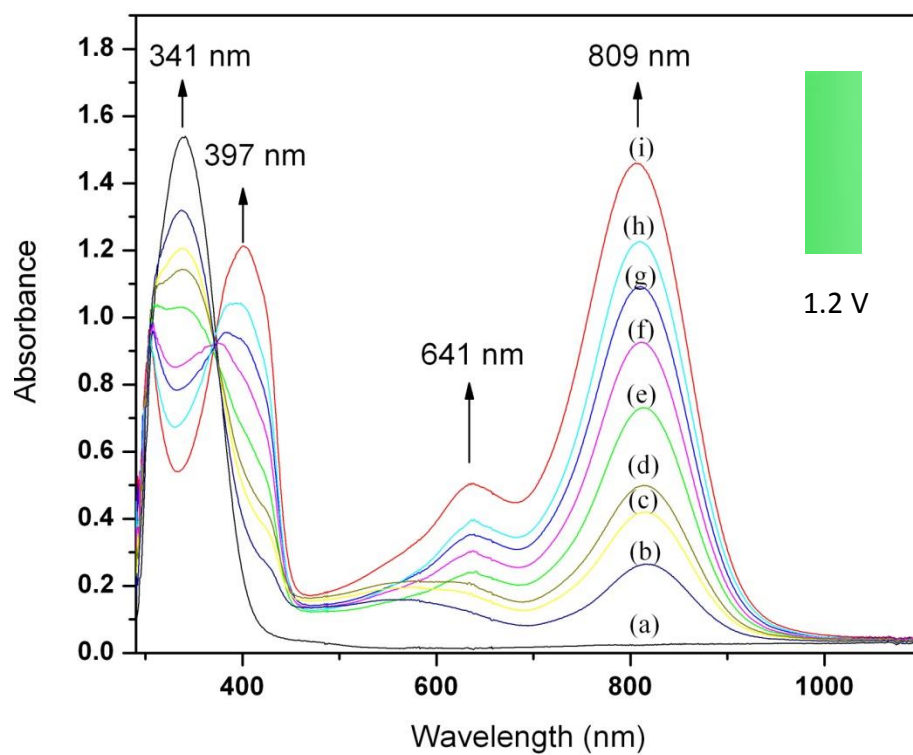


Fig. 6. Spectral changes of polyamide **7d** film on the ITO-glass substrate in 0.1 M TBAP/CH₃CN at different electrode potentials: (a) 0.0, (b) 0.60, (c) 0.69, (d) 0.78, (e) 0.88, (f) 0.97, (g) 1.07, (h) 1.17, and (i) 1.26 V.

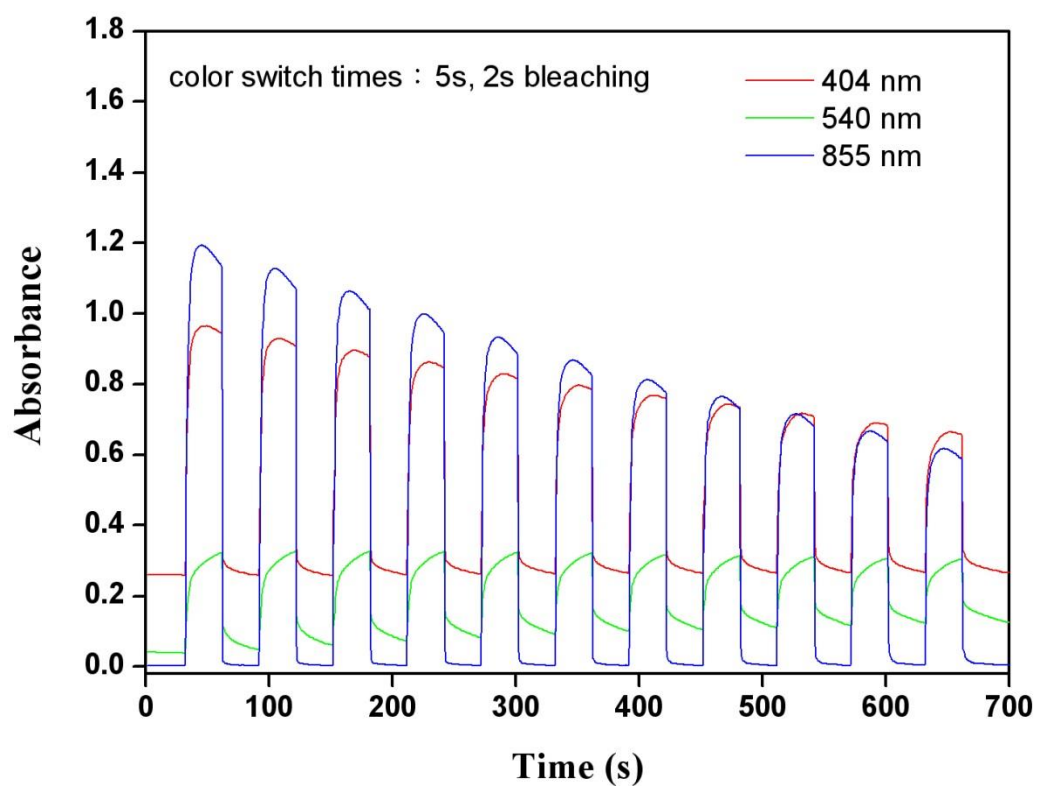


Fig. 7. Potential step absorptometry of polyamide **6a** in 0.1 M TBAP/CH₃CN by applying a potential step (0 V ⇌ 1.23 V).

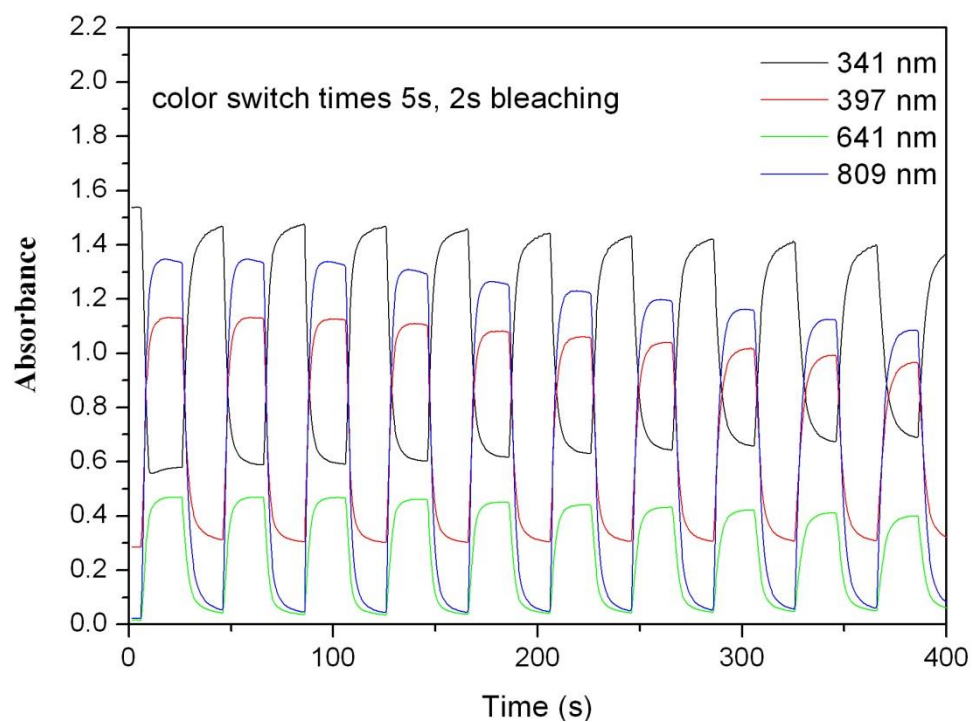
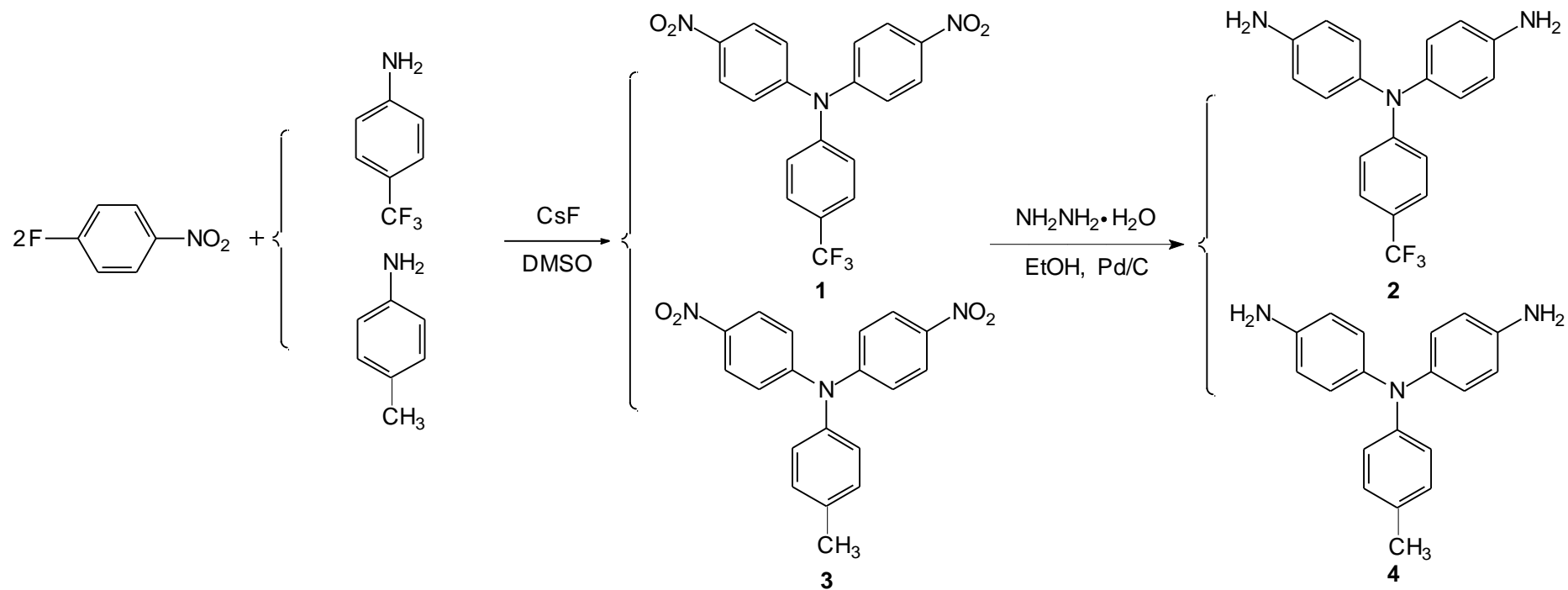
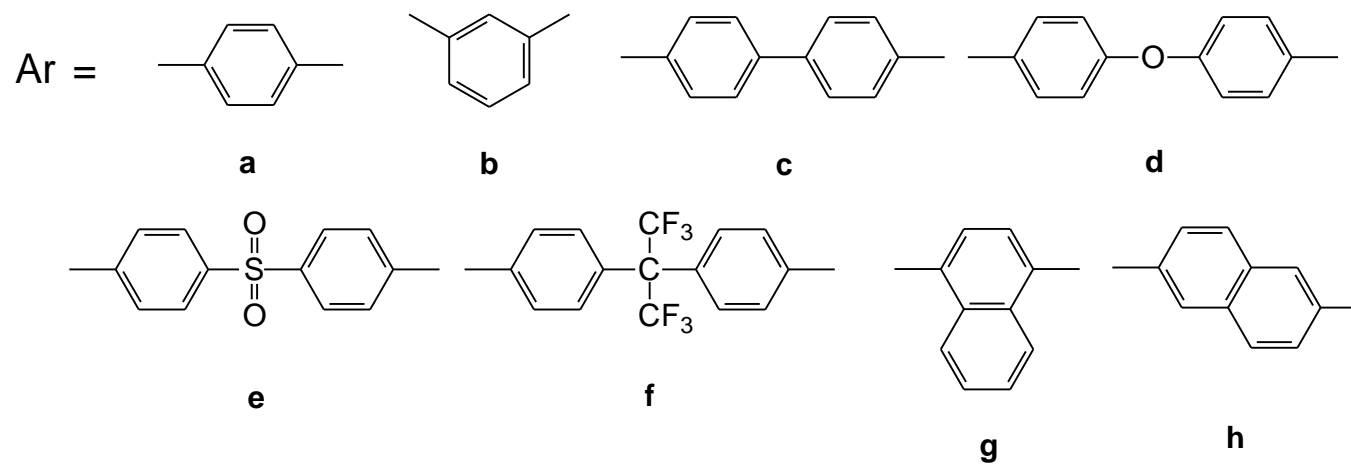
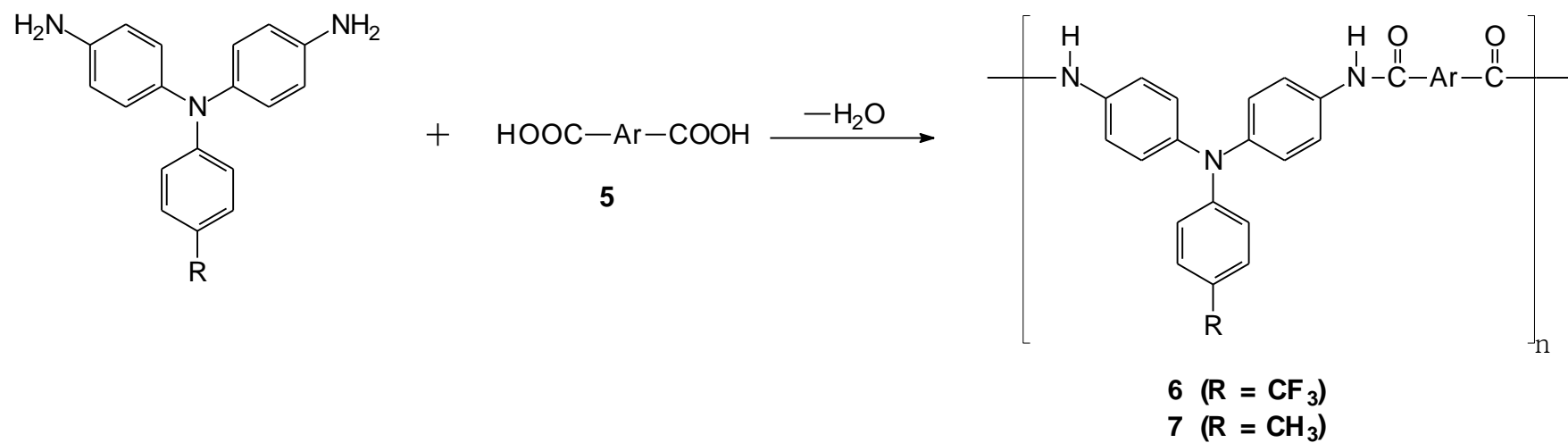


Fig. 8. Potential step absorptometry of polyamide **7d** in 0.1 M TBAP/CH₃CN by applying a potential step (0 V \rightleftharpoons 1.26 V).



Scheme 1. Synthesis routes to diamine monomers **2** and **4**.



Scheme 2. Synthesis of polyamides **6a–6h** and **7a–7h**.

Table 1: Inherent viscosity and solubility behavior of polyamides.

Polymer code	η_{inh} (dL/g) ^a	Solubility ^b					
		NMP	DMAc	DMF	DMSO	<i>m</i> -Cresol	THF
6a	0.98	+	+	+	+	–	–
6b	0.43	+	+	+	+	+h	–
6c	1.00	+	+	+	+	–	–
6d	0.91	+	+	+	+	–	–
6e	0.64	+	+	+	+	+h	–
6f	0.48	+	+	+	+	+	+
6g	0.43	+	+	+	+	+	–
6h	0.83	+	+	+	+	–	–
7a	1.31	+	+	+	+	+h	–
7b	0.42	+	+	+	+	+h	–
7c	1.69	+	+	+	+	+h	–
7d	0.98	+	+	+	+	–	–
7e	0.95	+	+	+	+	+h	–
7f	0.63	+	+	+	+	+h	–
7g	0.81	+	+	+	+	+h	–
7h	1.21	+	+	+	+	+h	–

^a Inherent viscosity of the polyamides measured at a concentration of 0.5 g/dL in DMAc at 30 °C.

^b Qualitative solubility was tested with 10 mg of a sample in 1 mL of the stirred solvent.

+ = soluble at room temperature; +h = soluble on heating at 100 °C; – = insoluble.

Table 2 Tensile properties of polyamide films.

Polymer code	Strength at break (MPa)	Elongation at break (%)	Initial modulus (GPa)
6a	87	17	1.6
6b	94	9	2.3
6c	110	49	2.7
6d	90	46	2.1
6e	92	13	2.1
6f	89	14	1.7
6g	95	7	2.3
6h	108	19	2.3
7a	103	12	2.5
7b	89	10	2.0
7c	126	20	2.9
7d	91	17	2.1
7e	76	7	1.8
7f	96	9	2.0
7g	117	8	2.6
7h	103	17	2.3

Table 3 Thermal properties of polyamides.^a

Polymer code	T_s ^b (°C)	T_d (°C) ^c at 10% wt loss		Char yield ^d (%)
		In air	In N ₂	
6a	289	450	467	67
6b	277	462	481	66
6c	302	513	530	69
6d	275	482	514	67
6e	285	484	495	65
6f	296	499	524	64
6g	277	483	511	70
6h	286	501	520	72
7a	294	518	526	72
7b	282	520	522	72
7c	310	532	542	74
7d	275	510	522	72
7e	308	485	493	66
7f	314	517	535	66
7g	281	513	499	72
7h	317	524	526	74

^a All the polyamide samples were heated at 300 °C for 1 h prior to TMA and TGA experiments.

^b Softening temperature, taken as the onset temperature of the probe displacement on the TMA trace at a scan rate of 10 °C/min.

^c Decomposition temperature, recorded via TGA at a heating rate of 20 °C/min and a gas flow rate of 30 cm³/min.

^d Residual weight percentages at 800 °C under nitrogen flow.

Table 4 Optical and electrochemical properties of the polyamides.

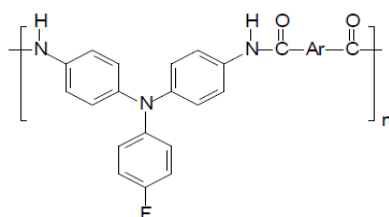
Polymer code	λ_{\max} (nm) ^a	λ (nm) ^a	$E_{1/2}$ (V) ^b	Band gap (eV) ^c	HOMO (eV) ^d	LUMO (eV) ^d
6a	342	409	1.00 (0.95)	3.03	5.36	2.33
6b	336	397	1.02 (0.95)	3.12	5.38	2.26
6c	300	414	0.97 (0.92)	3.00	5.33	2.33
6d	329	387	1.01 (0.99)	3.20	5.37	2.17
6e	317	443	1.03 (0.97)	2.80	5.39	2.59
6f	335	398	1.02 (0.97)	3.12	5.38	2.26
6g	320	399	1.03 (0.99)	3.11	5.39	2.28
6h	343	420	0.99 (0.91)	2.95	5.35	2.40
7a	294	428	0.86	2.90	5.22	2.32
7b	341	403	0.87	3.08	5.23	2.15
7c	301	418	0.84	2.97	5.20	2.23
7d	340	395	0.84	3.14	5.20	2.06
7e	323	445	0.88	2.78	5.24	2.46
7f	346	411	0.84	3.02	5.20	2.18
7g	318	426	0.83	2.91	5.19	2.28
7h	338	430	0.85	2.88	5.21	2.33

^a Read from the UV-Vis absorption spectra of the polymer films.

^b Oxidation half wave potential from cyclic voltammetry (vs. Ag/AgCl). Values in parentheses are data of the corresponding **8** series polyamides (from Ref. 50) having the same dicarboxylic acid residue as in the **6** and **7** series.

^c The data were calculated by the equation: Band gap = $1240/\lambda_{\text{onset}}$.

^d The HOMO energy levels were calculated from the oxidation $E_{1/2}$ value of CV diagrams and were referenced to ferrocene (4.8 eV relative to vacuum energy level; $E_{1/2} = 0.44$ V in CH₃CN). HOMO = $E_{1/2} + 4.8 - 0.44$ (eV); LUMO = HOMO – band gap.



Referenced **8** series polyamides: